Kinetics and Mass Transfer in a Fluidized Packed-Bed: Catalytic Hydrogenation of Ethylene

ROBERT J. FARRELL

and

EDWARD N. ZIEGLER

Department of Chemical Engineering
Polytechnic Institute of New York
333 Jay Street
Brooklyn, New York 11201

The kinetics of ethylene hydrogenation to ethane are studied in a 7.0 cm diameter fluidized packed-bed reactor. The fixed packing, 1.27 cm nickel on alumina catalyst, is used in conjunction with both $-48/+100$ mesh alumina and $-50/+170$ mesh glass inert fluidized particles. Reactant mixture is passed through the reactor at velocities sufficient to fluidize the inerts. Conversions from 0 to 91% are observed over the temperature range 56° to 261°C and flow rate range 10 to 800 cm³/s.

The mass transfer coefficient and reaction rate constant are simultaneously evaluated from integral conversion data. The mass transfer coefficient between the interstitially fluidized bed and the catalyst surface is correlated in dimensionless form as

$$N_{Sh} = 0.77\, N_{Re}^{0.418}\, N_{Sc}^{1/3}$$

The correlation is significant at the 95% confidence level (that is, $r = 0.59$, $\rho' > 0$.

Predictions of conversion using both the mass transfer coefficient correlation and a Langmuir-Rideal reaction expression are in good agreement with experimental data. The effects of contact time and catalyst diameter on conversion are also presented. Film diffusion influences become limiting at temperatures above 100°C at the velocities studied. Diffusional resistances were found to be important at Reynolds numbers below 100, at 186°C. No significant difference in reaction rate was found between fluidized alumina and glass inert particles under comparable operating conditions.

SCOPE

A packed fluidized bed utilizes inert packing to baffle catalyst particles which are fluidized in the interstices. This reduces bubble formation and gas bypassing while maintaining a high heat transfer rate. A similar technique has been used commercially for iron ore reduction. The pulverized ore is fluidized with hydrogen, using heated baffles as the inert packing. Volk et al. (1962) at Hydrocarbon Research, Inc., have demonstrated this process for reducing ferrous oxide to elemental iron for use in powdered metallurgy.

On the other hand, a fluidized packed bed utilizes inert fluidized particles in the interstices of a stationary catalyst for temperature control. A related technique has been used on a pilot scale by Gabor et al. (1966) at Argonne National Laboratory for the recovery of fissionable material from spent nuclear reactor fuels. Stationary uranium dioxide pellets are contacted with fluorine producing UF_6 from which the spent uranium is recovered. Inert particles of alumina are fluidized in the voids of the uranium dioxide pellets in order to maintain close temperature control.

Interstitial fluidized reactors lend themselves to applications in highly exothermic catalytic reactions, where temperature control is essential. Important reactions which should be considered include hydrogenations (benzene to cyclohexane, nitrobenzene to aniline, olefins to alkanes, and ammonia synthesis) oxidations (ethylene to ethylene oxide, *m*-xylene to naphthalene, and ammonia to nitric acid), or addition reactions such as acetylene plus hydrochloric acid to vinyl chloride.

While interstitially fluidized reactors are finding increasing applications in the process industries, diffusion controlled reaction rates have always been of importance. It is not uncommon to find that the reaction kinetics of heterogeneous catalytic reactions are controlled by the transport rates of both heat and mass to the catalyst pellets. Good catalysts tend to have diffusion limited rates even at moderate temperatures. Interstitially fluidized bed reactors have been used in the past to improve heat transfer rates. However, the effect of the fluidized particles on the rate of mass transfer to the packing has not been investigated previously. For this study, the Sherwood numbers are correlated with fluid Reynolds and Schmidt numbers. The transition from a reaction limited to a diffusion limited rate is also studied in the interstitially fluidized bed.

Correspondence concerning this paper should be addressed to Edward N. Ziegler. Robert J. Farrell is with Scientific Design Company, Inc., 2 Park Avenue, New York, New York 10016.

0001-1541-79-2512-0447-$01.05.

CONCLUSIONS AND SIGNIFICANCE

A numerical technique has been developed for the simultaneous evaluation of a reaction rate constant and a global mass transfer constant from integral rate data. This technique can be applied to rate data from other catalytic reactions in packed, fluidized, or interstitial reactors. The reaction rate for ethylene hydrogenation over the nickel catalyst in the present study is

$$r_{BS} = \frac{k_0 e^{-E/RT} C_{Ai} C_{Bi}}{1 + 619\, C_{Bi}} \quad \frac{\text{kg mole}}{\text{s} \cdot \text{m}^2 \text{ cat}}$$

where the rate constant $k_0 = 9.2 \times 10^5$ m^4/kg mole · s is higher than that for Koestenblatt's (1970) study, and $E = 43.1$ J/mg mole.

A correlation which adequately predicts the global bed to packing mass transfer coefficient in a fluidized packed bed is as follows:

$$N_{Sh} = b\, N_{Re}^{m}\, N_{Sc}^{1/3} \quad (r = 0.59,\ \rho' > 0)$$

where at the 80% confidence level

$$b = 0.770 \pm 0.310$$

$$m = 0.418 \pm 0.137$$

Conversions of ethylene in a fluidized packed bed can be accurately predicted using a kinetic model which combines the reaction rate equation and global mass transfer correlation.

As temperature is increased (50° to 180°C), the reaction mechanism transfers from predominantly reaction controlled to diffusion controlled at Reynolds numbers below 100.

No effect on overall conversion of ethylene to ethane was found upon switching from alumina to equally mobile glass fluidized particles in a packed bed of nickel catalyst at 180°C. This foretells of the difficulty of improving the overall rate of reaction by adding a highly adsorbent inert to the system (that is, at low temperature the rate is controlled by reaction whereas at high temperature diffusion controls, but adsorption capacity is low).

BACKGROUND

Fluidized Packed Beds

The packed-bed catalytic reactor with gaseous reactants is one of the mainstays of the chemical process industry. Reactors of this type are involved, for example, in the catalytic cracking of petroleum, ammonia synthesis, and removal of automobile pollutants. Many variations of the basic reactor have evolved because of the following inherent problems of this type of reactor: heat transfer difficulties, high investment cost, and diffusional limitations on reactor yield.

Poor heat transfer in packed beds produces nonuniform temperatures and hot spots resulting in a loss of selectivity and shorter catalyst life. In order to solve heat transfer difficulties, catalysts have, in many instances, been pulverized to a size suitable for fluidization. However, the gas-solid contact in a fluidized bed reactor is poorer than in a packed bed owing to bubble formation and gas bypassing. Because of this, yields in fluidized bed reactors are often lower than in packed-bed reactors. An earlier review of interstitial fluidization has been published by Ziegler (1972) in which a system involving the fluidization of small inert particles in the voids of a packed bed of larger catalyst or reactant particles has been referred to as a fluidized packed bed. Closely related is the system involving the fluidization of small catalyst or reactant particles in the voids of inert packed particles which to distinguish between the two is called a packed fluidized bed. Either of these systems can be used to enhance yield and selectivity of chemical reactions by providing close temperature control and reducing gas bypassing in gas-solid reactions.

Echigoya and Osberg (1960) investigated the use of a fluidized packed bed for the oxidation of ethylene oxide with silver catalyst at 230° to 270°C. They found that excellent temperature control could be achieved without the catalyst agglomeration problem encountered in fluidized bed reactors. Conversions were higher than for a conventional fluidized bed. Koestenblatt (1970) also found excellent temperature control while studying the mechanism of the hydrogenation of ethylene in a fluidized packed bed using nickel catalyst and inert fluidized particles at 30° to 90°C.

The excellent heat transfer characteristic of fluidized packed beds is brought about via the particle transfer mode. This mechanism of heat transfer to a fixed surface in a fluidized bed has been quantitatively shown by Ziegler and Brazelton (1964) to account for 80 to 95% of the total transport. Gabor (1965, 1966), has shown the effective thermal conductivity in interstitially fluidized beds to be directly proportional to the particle heat capacity.

Mass transfer from fixed surfaces to gas fluidized beds was investigated by Van Heerden et al. (1953) and by Ziegler and Holmes (1966). Using water and naphthalene evaporation studies, the latter investigators concluded that the mass transfer coefficient increases with the adsorptive capacity of the fluidized solid particles, confirming the Van Heerden group observations for the adsorption of naphthalene on both coke and Devarda's alloy in a fluidized bed. This effect is more easily detected at lower reaction temperatures, where particle adsorptive capacity is higher.

Gas mixing in fluidized packed beds has been studied by Koo (1971). Using data obtained in the range $3 < N_{Sc} \cdot N_{Re} < 20$, he found that the ratio of variances in packed and fluidized packed beds approached unity in value. This suggests that reaction conversion analysis of fluidized packed beds might be handled in a manner similar to packed beds. Koestenblatt (1970) showed that at conversions of 60% or less, the residence time required, as predicted by plug flow analyses, differed by less than 10% from the observed values. Above 60%, greater variations did occur, but variations were still less than 16% at 90% conversion.

Ethylene Hydrogenation

Extensive work on hydrogenation of ethylene on nickel apropos packed-bed behavior may be summarized using

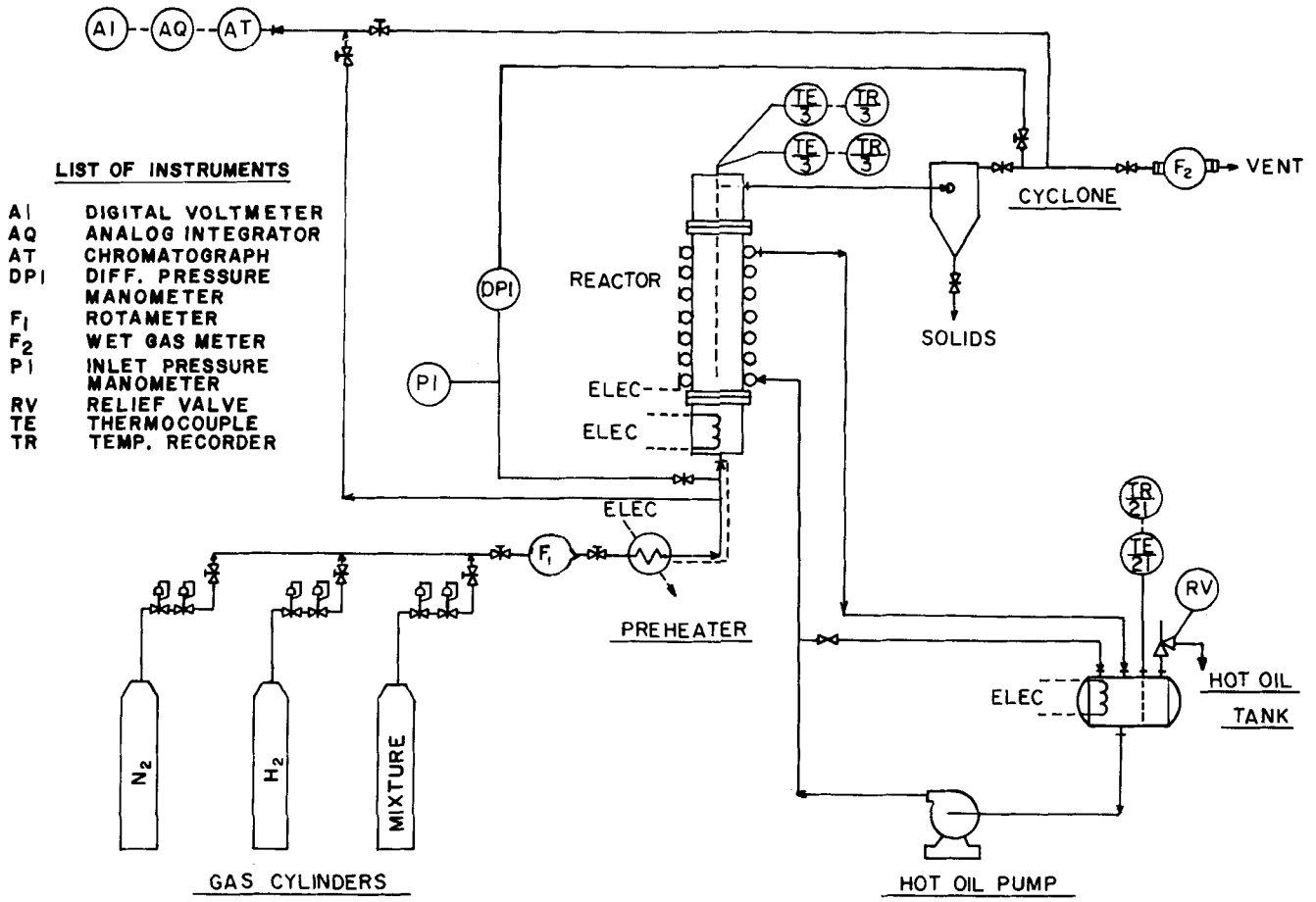

Fig. 1. Fluidized packed bed reactor system.

the results of illustrative studies as follows:

1. The rate of the reaction appears to be controlled by an adsorbed hydrogen and gas phase ethylene step (see Jenkins and Rideal, 1955; Pauls et al., 1959, for example) and is best described by an expression of the form

$$\text{rate} = \frac{k_1 P_A P_B}{1 + k_2 P_B}$$

2. The activation energy values measured below 150°C fall between 40.6 and 48.6 J/mg mole. Above 150°C, Fulton and Crosser (1965) observed a shift in the kinetic mechanism to an activation energy of 8.2 J/mg mole. Gioia and Green (1967) did not observe this change in mechanism when recalculating the data based on low Reynolds number j_D and j_H correlations.

3. Fulton and Crosser found that external diffusional resistances influence the rate of reaction at 93°C with catalyst diameters greater than 0.05 cm. Internal diffusional resistances have been shown to be small.

The hydrogenation of ethylene has also been investigated in interstitially fluidized bed reactors. Kato et al. (1974, 1969) correlated conversions obtained in a packed fluidized bed (fluidized nickel catalyst with stationary glass spheres and with wire mesh packing). Using a two-phase model, they obtained agreement at an empirical value of 0.2 for the fraction of catalyst in the bubble phase. Koestenblatt and Ziegler (1971) studied the kinetics in a fluidized packed bed of stationary nickel on alumina catalyst with fluidized glass inerts. They obtained a kinetic expression comparable to that found for packed beds. In addition, it was shown that catalyst activity can be temporarily increased or decreased upon switching from hydrogen to ethylene rich reactant mixtures, respectively.

EXPERIMENTAL APPARATUS AND PROCEDURES

In this work, the objectives are to study experimentally the catalytic hydrogenation of ethylene in a fluidized packed bed under diffusion controlled conditions to determine how the reaction rate varies with system parameters. Figure 1 is a schematic diagram of the experimental equipment used, and Figure 2 the reactor detail. The reactor is packed with ½ in. (1.27 cm) alumina blanks, ½ in. (1.27 cm) catalyst particles, and −48/+170 mesh inert particles (see Table 1). At reactant mixture flow rates greater than a superficial velocity of approximately 83.3 cm³/s, the inert particles become fluidized.

The product gases leaving the reactor disengaging section pass through a cyclone separator (major dimensions 5.1 by 20.3 cm high) to a vent. Entrained inert particles are periodically drawn from the bottom of the cyclone. The gas discharge line is provided with both a pressure tap and a gas sampling connection. A wet test meter located at the vent measured the flow of product gases. A nitrogen purge system is provided for use during start-up and shutdown, and a hydrogen feed system is also provided for in-situ catalyst reduction and reactivation. Reaction temperature is controlled (±1.5°C) between 56° to 261°C by means of a hot oil circulation system. The reaction temperature was measured at the catalyst surface by thermocouples which were fixed with a drop of epoxy resin into a hole previously formed by sand blasting.

The catalyst was prepared by depositing nickel nitrate on the nonporous alumina carrier and then calcining to obtain a nickel oxide on alumina catalyst. The method used is similar to that described by Pauls et al. (1959) and Koestenblatt (1970). Catalyst reduction from nickel oxide to nickel was carried out in-situ with 23.6 cm³/s of hydrogen at 250° to 270°C for 24 hr.

Gas samples are analyzed by means of gas-liquid chromatography. A Perkin-Elmer 154L gas chromatograph is used to determine the composition of the feed and product streams. The 0 to 1 mV output from the GLC is sent to a model TR-10 analogue computer, where the signal is integrated with re-

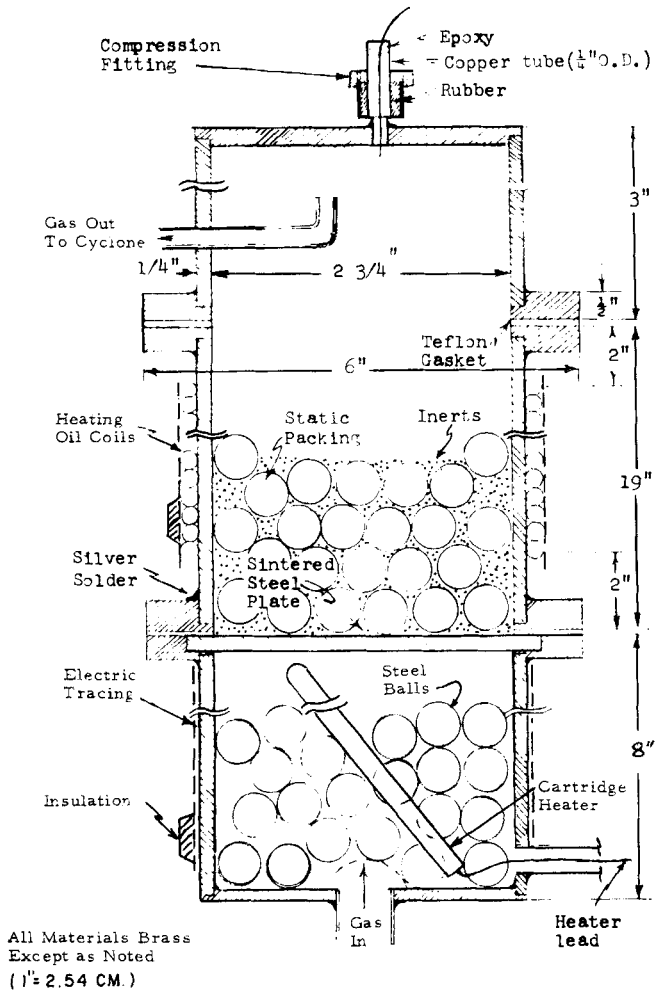

Fig. 2. Reactor schematic.

TABLE 1. RANGE OF VARIABLES INVESTIGATED

Variable	Range
Packed catalyst size	0.5 in. (1.27 cm)
Inert particle size	50-170 mesh
Inert particle type and shape factor in parentheses	Glass microspheres (1.0); Alcoa powdered alumina F-1 (0.6); Union Carbide activated carbon MBV (0.6)
Temperature	56°-261°C
Amount of catalyst	0.043-0.253 kg
Superficial flow rate	10-800 cm^3/s

spect to time. The integrated output signal from the analogue computer is flashed on a digital voltmeter. The equivalent peak area for each component is found by recording the change in the digital reading during that component's evolution. The reading is compared with those of a previously calibrated standard cylinder to give the sample composition. It was found that this procedure was accurate, provided measurements of GLC baseline drift were made before and after each sample. Using this set-up, analytic results were obtained quickly with the time required to complete a sample averaging around 15 to 20 min.

The sampling technique used is similar to that described by Sinfelt (1968). Sampling in this manner minimizes catalyst deactivation and poisoning effects by utilizing hydrogen regeneration after each sample. In addition, the catalyst is discarded after a maximum of seven samples or 70 min total contact time to also minimize catalyst aging.

Table 1 is a summary of the range of variables studied in this work. The gas mixture flow rate was an important limitation, with the lower rate being that required for fluidization of the inerts while the upper limit was defined by the economic use of the reactant mixture.

EXPERIMENTAL RESULTS

Both alumina and glass inert particles were used. The glass mixture was chosen as 70% −50/+70 mesh and 30% −120/+170 mesh to give an average particle size which from calculated estimates would have fluidization properties close to those of the −48/+100 alumina. The minimum fluidization velocity obtained for alumina was 118 cm^3/s and for glass was 66 cm^3/s using nitrogen at 25°C and 1.08×10^5 N/m^2 pressure.

Rate Data

Using both inert particle mixtures, a total of sixty nine experimental runs were made on the hydrogenation of ethylene.

Assuming plug flow in a tubular reactor, the material balance across a differential element is

$$F_B\, dX_B = (-r_B)\, dW \tag{1}$$

Equation (1) describes the specific rate of disappearance of ethylene. An average rate of disappearance across the reactor may be defined for convenience as

$$r_{Bavg} \equiv \frac{\Delta X_B}{\Delta\left(\frac{W}{F_B}\right)} \tag{2}$$

Such rates were used for *preliminary* determinations and analysis only. Table 2 gives the conversion data for typical runs along with the average reaction rate as defined by Equation (2). Initial runs were taken over the course of 3 mo, with the same batch of catalyst being reactivated before each day's series of runs. Unlike the initial runs, a fresh batch of catalyst was used for each day's series of runs for data such as those presented in Table 2.

Also, after the initial runs, in which the catalyst was pretreated with reactant mixture, it was decided to switch to hydrogen pretreatment with regeneration after each sample. The frequent return to a hydrogen atmosphere reduces catalyst poisoning and maintains a higher catalyst activity level. The average reaction rate for the initial runs was typically one order of magnitude lower than for the remainder of the data.

A study of the effect of temperature for various treated catalysts is graphically illustrated in Figure 3. Here, a plot of the average reaction rate vs. reciprocal temperature is drawn from the data of Table 2, the initial runs and the results of Koestenblatt and Ziegler (1971). It is apparent that for the data of the present study, little change of rate occurs with temperature. Koestenblatt's reaction rates, on the other hand, increase sharply as the temperature increases.

The lower catalyst activity encountered by Koestenblatt (1970) and the observed Arrhenius temperature behavior are consistent with his conclusion that a surface reaction (nonporous catalyst) controlled the rate. At the higher catalyst activities observed in the current study, the lack of variation of average reaction rate with temperature is consistent with a predominantly film diffusion controlled step, to be discussed later. Upon comparison of rate data for glass and alumina inerts under similar inlet conditions, no significant difference in conversion was found. Experiments with fluidized activated carbon resulted in negligible conversion and were discontinued. Possibly, air was adsorbed by the carbon particles prior to catalyst reduction, ultimately inhibiting the hydrogenation reaction.

TABLE 2. TYPICAL EXPERIMENTAL DATA-ALUMINA INERTS

Reactor loading
Size of inerts: −48 + 100 mesh
Kgs of inerts: 0.501
Size of catalyst: 0.50 in. (1.27 cm)
Kgs of catalyst: 0.0745

Run	Temp., °C	Pressure-$N/m^2 \times 10^{-5}$ In	Out	Super vel., cm^3/s	Molar rate in (kg mole/s) $\times 10^6$ C_2H_4	H_2	C_2H_6	Percent conver.	Rate from Equation (2) $\times 10^6$ kg mole/s · kg cat
1	177.9	1.600	1.560	766.0	9.202	23.149	0.367	3.14	3.88
2	181.0	1.123	1.086	449.6	3.766	9.467	0.150	13.99	7.07
3	186.1	1.070	1.033	291.6	2.303	5.789	0.092	32.34	10.00
4	194.6	1.036	1.003	79.8	0.599	1.506	0.024	86.26	6.93
5	170.6	1.223	1.186	577.3	5.389	13.548	0.215	5.43	3.93
6	171.2	1.340	1.302	683.9	6.985	17.558	0.278	5.94	5.57
7	173.4	1.050	1.013	180.5	1.438	3.615	0.057	64.75	12.50

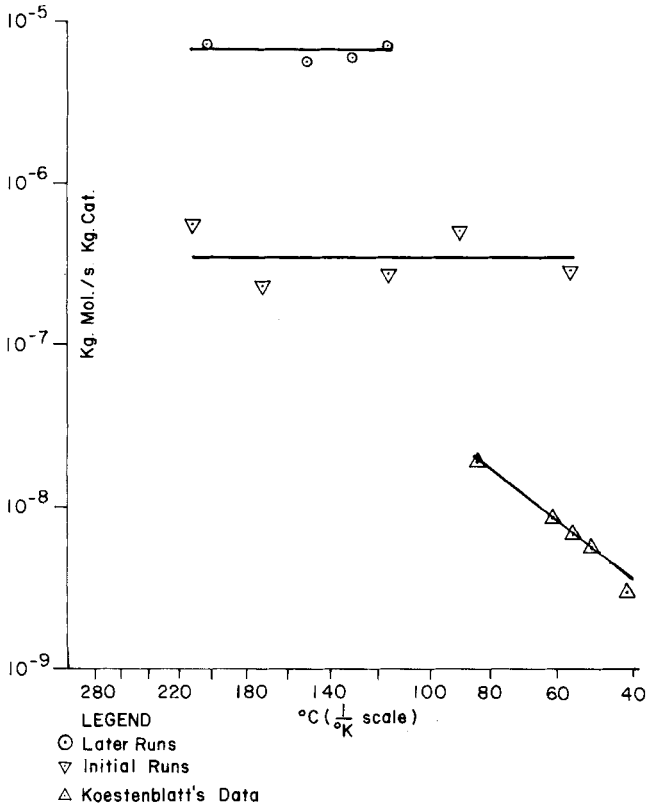

Fig. 3. Effect of temperature on conversion for various catalysts.

ANALYSIS OF DATA

Although preliminary analysis of the average reaction rates suggested that gas film diffusion may influence the overall reaction rate, the degree of diffusion had yet to be established. Initial attempts to correlate the data using a 100% diffusion controlled model succeeded partially. It was felt that experimental data, especially at high Reynolds numbers, were probably observed under conditions where neither surface reaction nor film diffusion control the overall rate. A comprehensive rate equation was developed allowing for the influence of both steps. The data were analyzed by integrating this equation using a plug flow reactor model. This is justified on the basis of conversion calculations of Koestenblatt (1970) and gas mixing findings of Koo (1971) mentioned earlier. The constants in the rate equation are then found by best fitting the integrated data to a dimensionless mass transfer equation analogous to the Nusselt form of heat transfer equation. The resulting equation for film diffusion rates provides a measure of mass transfer in a fluidized packed bed.

Development of Model

For the nonporous catalyst used in this study, internal diffusional effects on the rate are insignificant. Therefore, based on the unit exterior surface of the catalyst particle, the mass flux of ethylene and hence overall local rate (r_{BS}) can, in any instance, be expressed as

$$r_{BS} = -\frac{1}{S_{ext}}\frac{dN_B}{dt} = k_{GB}\,(C_{Bb} - C_{Bi}) \qquad (3)$$

In the case of mass transfer control, the reaction rate is considered to proceed so fast that C_{Bi} in Equation (3) falls to a value of zero. If, in fact, ethylene diffusion does not control the rate, C_{Bi} will have some nonzero value.

Koestenblatt's surface reaction rate equation form is used, but a catalyst activity factor η allows for the higher reaction rates obtained for the catalyst of this study. The use of the catalyst activity factor is similar to that of Sane et al. (1974) in modeling the catalytic hydrogenation of butadiene. Incorporating this into Koestenblatt's surface reaction rate equation results in the reaction rate equation

$$r_{BS} = \frac{\eta k_R\, C_{Ai}\, C_{Bi}}{1 + K_A\, C_{Bi}} \qquad (4)$$

where for 1.27 cm catalyst (8.02×10^{-5} m^2 external surface/g) the values of the constants are

$$k_R = 1.77 \times 10^4\, e^{-43.1/RT}\,\frac{m^6}{\text{kg mole} \cdot s \cdot m^2\ \text{cat}}$$

and

$$K_A = 619.0\,\frac{m^3}{\text{kg mole}},$$

respectively. If this surface reaction controls the rate, $C_{Ai} = C_{Ab}$ and $C_{Bi} = C_{Bb}$, and Equation (4) may be expressed in terms of bulk phase concentration values.

At steady state, the mass flux of ethylene toward the catalyst interface is equal to the mass flux of hydrogen toward the catalyst interface, for the equimolar stoichiometry. Hence, C_{Ai} may be found in terms of bulk diffusivities and C_{Bi}. The value of C_{Bi} is then obtained by setting the rate of mass flux to the catalyst surface equal to the rate of surface reaction, Equations (3) and (4), respectively:

$$C_{Bi} = \frac{-\gamma + (\gamma^2 + 4K_A C_{Bb} + 4\alpha R' C_{Bb})^{1/2}}{2K_A + 2\alpha R'} \qquad (5)$$

where

$$k_R' = \eta k_R, \quad \alpha = \frac{k_R'}{k_{GB}}, \quad R' = \frac{D_{BM}}{D_{AM}}, \quad \text{and}$$

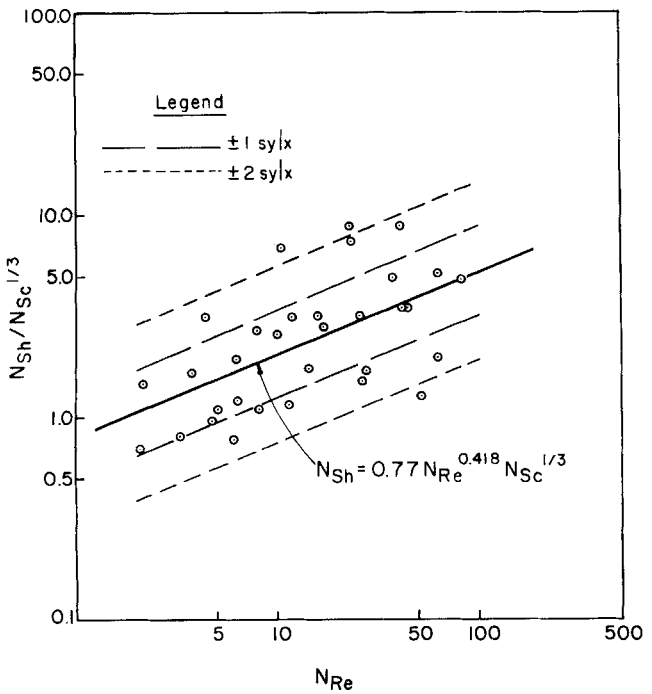

Fig. 4. Results of regression analysis.

$$\gamma = (\alpha C_{Ab} + 1 - K_A C_{Bb} - R' \alpha C_{Bb})$$

The resulting expression for C_{Bi} is substituted back into the right-hand side of Equation (3) to give a rate which is expressed as a function of bulk concentrations, alone. By taking a material balance across the catalyst bed and integrating, we get

$$\frac{\rho_p}{a_p} \int_{F_{B0}}^{F_B} \frac{dF_B}{-r_{BS}(C_B, k_R', k_{GB})} = W \qquad (6)$$

where

$$r_{BS} = k_{GB} \left(C_{Bb} - \frac{-\gamma + (\gamma^2 + 4K_A C_{Bb} + 4\alpha R' C_{Bb})^{1/2}}{2K_A + 2\alpha R'} \right) \qquad (7)$$

Before Equation (6) can be integrated, r_{BS} must be expressed as a function of F_B. This can be accomplished by using a mass balance across the reactor and the reaction stoichiometry. For details, the reader is referred to the work of Farrell (1977).

In Equation (6), ρ_p and a_p are known from the catalyst properties, other inlet concentrations and properties are obtained from gas samples, and K_A is known from Koestenblatt's reaction rate equation. Hence, only two constants, the surface reaction velocity and the gas phase mass transfer coefficient, k_R' and k_{GB}, respectively, remain to be best fit.

One may infer from Equation (6) that for each estimated k_R' there is a unique best value of k_{GB}. It is assumed for convenience that the catalyst activity η is a constant for all the data of the current study. This is probably a good assumption, since the catalyst is reactivated often. The pretreatment used in the current study leads to a higher activity than that of Koestenblatt and Ziegler's (1971) study.

The variable k_{GB} is dependent on numerous factors such as the relative velocity of the gas, the size of the catalyst particle, and gas properties. These factors have been correlated in packed and fluidized beds. No correlations have as yet been developed in fluidized packed beds. On the basis of the experimental evidence and semiempirical equations developed in packed and fluidized beds, it is assumed for the present system that k_{GB} may be correlated by an equation of the form $N_{Sh} = N_{Sh}[N_{Re}, N_{Sc}]$ using a power law:

$$\frac{k_{GB} d_p}{D_{BM}} = b \left(\frac{d_p V \rho_G}{\mu_G} \right)^m \left(\frac{\mu_G}{\rho_G D_{BM}} \right)^n \qquad (8)$$

For the data in this study, there is little change in the Schmidt number N_{Sc}. It was decided to choose $n = 1/3$ rather than analyze the Schmidt number variation statistically. Bar-Ilan and Resnick (1957) investigated naphthalene in air evaporation in packed beds and found this power to be valid for $2 < N_{Re} < 200$.

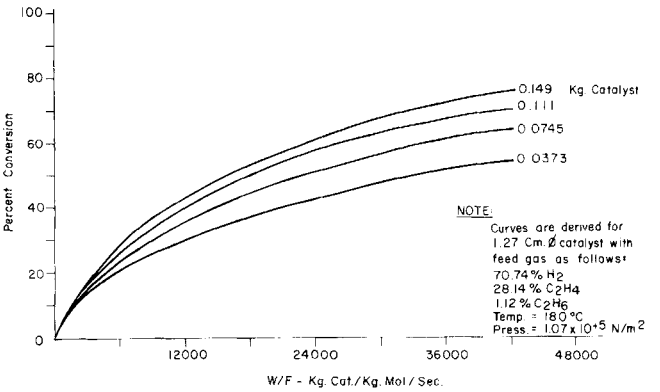

Fig. 5. Test for film diffusion effect.

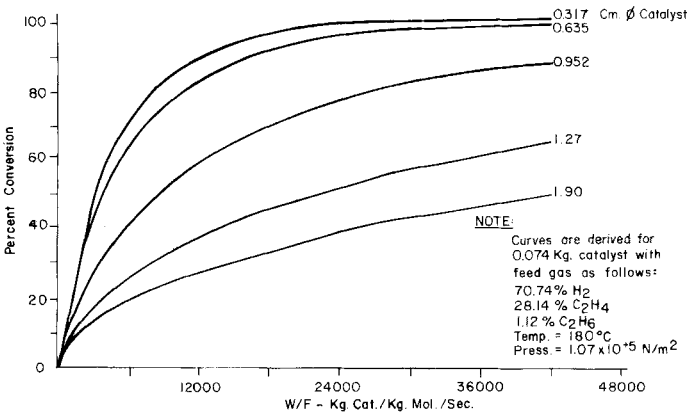

Fig. 6. Effect of catalyst diameter on conversion.

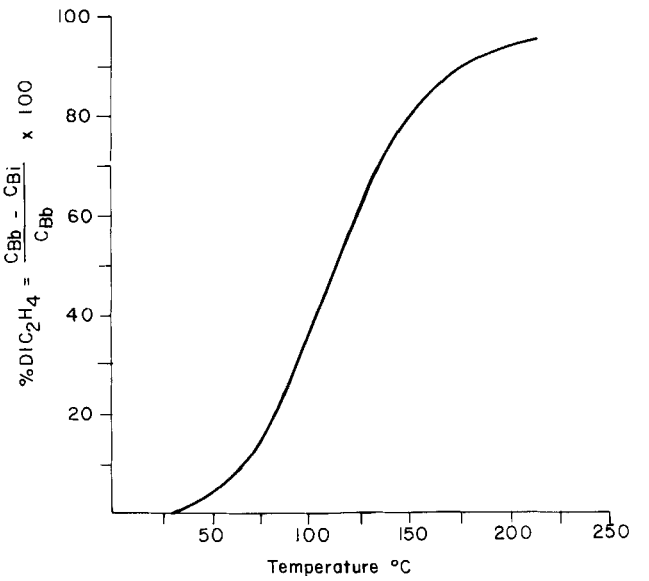

Fig. 7. Relative degree of diffusion control vs. temperature.

The gas mixture viscosity and diffusivity are calculated according to the prediction methods for gas mixtures at low density outlined in Bird, Stewart, and Lightfoot (1960). In addition, the diffusivity of an individual component in the gas mixture is found using the method of Wilke (1950).

A trial and error technique may be applied to Equation (6) for the purpose of estimating the relevant parameters. A value of η is assumed, and k_R' is calculated for the data. Using the values of k_R', Equation (6) is used to find a value of k_{GB}. The k_{GB}'s are correlated by Equation (8), and the precision of the correlation is estimated. These steps are repeated using different η values until the best correlation is obtained as described below.

A least-squares analysis is performed on the logarithm of Equation (8) which may be written in the symbolic linear form $y = b' + m'x$. The precision of the correlation is measured, for convenience, by the value of the reduced error, defined as

$$\mathrm{ERR}_r = \frac{S\,\bar{y}\,|\,\bar{x}}{\bar{y}'}$$

where $S\,\bar{y}\,|\,\bar{x}$ is the standard error of the estimate at the mean value of x, and $\bar{y}'$ is the predicted y value using the regression equation at the mean x value. The best fit of k_R' and k_{GB} in Equation (6) is based on the value of η which gives the minimum value of the reduced error (ERR_r). Most of the scatter in the dimensionless correlation is expected at the extremities of Reynolds number, and it was for this reason that it was decided to minimize (ERR_r) as the correlation criteria. High Reynolds number scatter arises from the assumption of a constant η for data points which are predominantly surface reaction rate controlled. Low Reynolds number points generally exhibit greater scatter, since higher conversions result in lower exit ethylene concentrations, thereby magnifying analytical errors.

Results of the Regression Analysis

The regression analysis of all the data except for a few discarded values are presented in graphical form in Figure 4. This represents the thirty-two point correlation which is felt to be the best for the data studied.

In choosing thirty-two points for the correlation data base, one abnormally high reaction rate point was eliminated along with the five highest deviation points which were coincidentally taken on the same 2 days. The justification for discarding these points is based on the fact that they are generally high Reynolds number points which tend to be reaction controlled, thereby more sensitive to the assumption of a constant catalyst activity for all runs. The correlation can be expressed as

$$\frac{k_{GB}d_p}{D_{BM}} = 0.77\left(\frac{d_p V \rho_G}{\mu_G}\right)^{0.418}\left(\frac{\mu_G}{\rho_G D_{BM}}\right)^{1/3} \qquad (\pm 40\%,\quad 1Sy\,|\,x) \qquad (9)$$

Using standard methods outlined in Crow et al. (1964) and discussed by Farrell (1977), it is found that the correlation is significant at the 95% level (that is, $r = 0.59$, $\rho' > 0$). At the 80% confidence level, $b = 0.77 \pm 0.31$, and $m = 0.418 \pm 0.137$.

While there is considerable scatter in the correlation of Figure 4, this is typical of mass transfer measurements in fluidized packed beds (Gabor, 1978). The Sherwood numbers found in this study are similar in magnitude to those found by Resnick and White (1949) who studied the sublimation of naphthalene for Reynolds numbers 0.62 to 121. These values are lower than both single-sphere and packed-bed correlations. In this study, it is possible that the larger inert particles are no longer fluidized at lower Reynolds numbers. These particles may agglomerate in the interstices of the catalytic packing, rendering some surface ineffective for mass transfer. Alternately, packing of the inerts may reduce the concentration gradients, thereby reducing mass transfer, as discussed by Cornish (1965). The assumption of plug flow should lead to lower than actual N_{Sh} (usually $< 10\%$ lower). Oddly, for five of the six cases run at higher than 50% conversion, where the plug flow assumption should lead to the greatest negative deviations, the N_{Sh} values were higher than those predicted by the correlation. This partially justifies the assumption of plug flow in the analysis.

The reaction rate equation incorporating the catalyst activity modification of Koestenblatt's expression gives, for this study

$$r_B = \left(\frac{a_p}{\rho_p}\right) r_{BS} = \left(\frac{a_p}{\rho_p}\right)\left(\frac{9.2 \times 10^5\, e^{-43.1/RT} C_{Ai} C_{Bi}}{1 + 619.0\, C_{Bi}}\ \frac{\text{kg mole}}{\text{s} \cdot \text{m}^2\,\text{cat}}\right) \qquad (10)$$

The two Equations (9) and (10) can now be combined to give an overall rate equation of the form of Equation (6) which can now be used to predict the conversion of ethylene.

EFFECT OF VARIABLES ON CONVERSION

Space Time and Catalyst Size

A series of numerically integrated solutions of Equation (6) were made to predict the variation of conversion with catalyst mass and gas flow rates. Using the measured inlet properties of Table 2, run 3, as a convenient base case (having intermediate conversion), the mass of catalyst was numerically varied from 0.037 to 0.149 kg (that is, fourfold), and the flow rate was varied over a time factor (W/F) of 0 to 45 000 kg catalyst/(kg mole fed/s). If we hold the temperature, pressure, and feed compositions constant at the values for the base case, Figure 5 demonstrates the extent of conversion vs. contact time obtained. This plot can be used to determine the region of film diffusion control. Where the curves are not coincidental ($W/F > 1\,500$, lower N_{Re}), surface film effects are important. The conversion vs. contact time curves may also be developed for other catalyst diameters by using the proper a_p and ρ_p values in Equation (6). Figure 6 shows the predicted conversion vs. contact time relationship for various catalyst sizes assuming a charge of 0.0745 kg. As diameter is decreased, the mass transfer coefficient increases appreciably, resulting in increasing surface rate domination.

Temperature

The effect of temperature on the reaction mechanism can also be found by using Equation (6) to determine the predicted conversion. This was done for temperatures of 25° to 250°C using the feed rate of the base run 3. As the temperature increases, the reaction mechanism becomes progressively more diffusion controlled. The degree of diffusion control can be expressed as the difference in the bulk phase ethylene concentration and the catalyst interface ethylene concentration over the bulk concentration at the reactor inlet. This quantity may be defined as

$$\frac{C_{Bb} - C_{Bi}}{C_{Bb}} = DIC_2H_4 \qquad (11)$$

A plot of the predicted values of this quantity vs. tem-

perature is shown in Figure 7. At 100°C, this value is 0.35. As temperature increases, however, its value increases to 0.94 at 200°C and then to 0.98 at 250°C. At 50.5°C, where Koestenblatt's data was correlated, $DIC_2H_4 = 0.04$, indicating a reaction controlled rate. For this study at about 180°C, $DIC_2H_4 = 0.83$, indicating a diffusion controlled rate.

As previously mentioned, no trend was observed upon comparing alumina and glass inerts under comparable operating conditions. Adsorption rates at the catalyst surface probably depend on two parallel paths, one via conveyance of adsorbed molecules by particles moving from the interstices to the packing surface and the other via gas phase diffusion alone. If fluidized particle adsorptivity of reactant mixture molecules is high, the conveyance mechanism predominates. However, high temperature may reduce the equilibrium adsorptive capacity of solids to a negligibly low value. Possibly this is why alumina, normally a better adsorbent than glass at room temperature, had little effect on the overall rate at the elevated temperatures of the current study. Enhancement of the rate probably occurs only in situations where the catalyst is effective at temperatures which are low enough to attain appreciable adsorption on the particles.

ACKNOWLEDGMENT

This manuscript is partly taken from the dissertation of R. J. Farrell submitted to the faculty of the Polytechnic Institute of New York in partial fulfillment of the requirements for the degree Ph.D. (Chem. Eng.), 1977.

NOTATION

a_p = particle area factor, L^2/particle
b = regression coefficient in Equation (8)
C_{Ab}, C_{Bb} = molar concentration of A and B in bulk phase, moles/L^3
C_{Ai}, C_{Bi} = molar concentration of A and B at catalyst interface, moles/L^3
d_p = fixed packing diameter, L
D_{im} = effective binary diffusivity of component i in the mixture, L^2/t
D_{ij} = binary diffusivity for system of i and j, L^2/t
DIC_2H_4 = reduced concentration gradient = $(C_{Bb} - C_{Bi})/C_{Bb}$
E = activation energy, ML^2/t^2
ERR_r = reduced error = $(S\,\bar{y}\,|\,\bar{x})/\bar{y'}$
F = molar flow rate of bulk gas phase, moles/t
F_{Ao}, F_{Bo} = molar flow rate of component A or B into reactor, moles/t
j_D = Chilton-Colburn j factor for mass transfer
j_H = Chilton-Colburn j factor for heat transfer
K_A = adsorption equilibrium constant, L^3/mole
k_{GA}, k_{GB} = gas phase mass transfer coefficient of A and B to exterior catalyst surface, L/t
k_R = surface reaction rate constant, L^6/mole · t L^2 cat
k_R' = modified reaction rate constant = ηk_R, L^6/mole · t L^2 cat
k_1, k_2 = constants at constant temperature
m = exponent of N_{Re} in Equation (8)
n = exponent of N_{Sc} in Equation (8)
N_B = moles C_2H_4
N_{Re} = Reynolds number = $d_p V \rho_G/\mu_G$
N_{Sc} = Schmidt number = $\mu_G/\rho_G D_{BM}$
N_{Sh} = Sherwood number = $k_{GB}d_p/D_{BM}$
P = pressure, M/Lt^2
R = gas constant, $ML^2/t^2\,T$ · mole
R' = ratio of diffusivities, D_{BM}/D_{AM}
r = correlation coefficient
r_B = rate of reaction based on mass of catalyst, mole/tM_{cat}
r_{Bavg} = average rate of reaction as per Equation (2), mole/tM_{cat}
r_{BS} = rate of reaction based on exterior catalyst surface, mole/tL^2_{cat}
S_{ext} = exterior catalyst surface, L^2
$Sy|x$ = standard error of estimate
$S\,\bar{y}\,|\,\bar{x}$ = standard error of predicted y at the mean x value
T = temperature
t = time
V = superficial velocity, L/t
W = weight of catalyst, M
x = arbitrary abscissa
X_B = moles ethylene converted/mole ethylene in feed
y = arbitrary ordinate
$\bar{y'}$ = predicted value of y at mean x value

Greek Letters

α = ratio of k_R'/k_{GB}, Equation (5), L^5/mole · L^2 cat
γ = defined in Equation (5)
ρ' = true population correlation coefficient
ρ_g = gas density, M/L^3
ρ_p = particle weight factor Equation (10), M/particle
μ_G = gas viscosity, M/LT
η = catalyst activity factor

Subscripts

A = hydrogen
B = ethylene
i = interface
units: L-length, M-mass, t-time, T-temperature; if no units, quantity is dimensionless.

LITERATURE CITED

Bar-Ilan, M., and W. Resnick, "Gas Phase Mass Transfer in Fixed Beds at Low Reynolds Numbers," *Ind. Eng. Chem.*, 49, 313 (1957).

Bird, R. B., W. E. Stewart, and E. N. Lightfoot, *Transport Phenomena*, Wiley, New York (1960).

Cornish, A. R. M., "Note on Minimum Possible Rate of Heat Transfer from a Sphere when other Spheres are Adjacent to It," *Trans. Inst. Chem. Engrs.*, 43, T332 (1965).

Crow, E. L., F. A. Davis, and M. W. Maxfield, *Statistics Manual*, Dover, New York (1964).

Echigoya, E., and G. J. Osberg, "Using Silver Catalyst Coated Strips in an Inert Fluidized Bed," *Can. J. Chem. Engrs.*, 38, 108 (1960).

Fair, J. R., "Kinetics of the Catalytic Hydrogenation of Light Olefins," Ph.D. thesis, Univ. Texas (1955).

Farrell, R. J., "Kinetics and Mass Transfer in a Fluidized—Packed Bed: Catalytic Hydrogenation of Ethylene," Ph.D. thesis, Polytech. Inst. N.Y. (1977).

Fulton, J. W., and O. K. Crosser, "Influence of Catalyst Particle Size on Reaction Kinetics, Hydrogenation of Ethylene on Nickel," *AIChE J.*, 11, 513 (1965).

Gabor, J. D., Personal communication (1978).

———, "Fluidized Packed Beds," *Chem. Eng. Progr. Symposium Ser.*, 62, 32 (1966).

———, "Lateral Transport in a Fluidized Packed Bed. Solids Mixing," *AIChE J.*, 11, 127 (1965).

Gioia, F., and D. W. Green, "Effects on Internal and External Diffusion for the Hydrogenation of Ethylene in a Porous Nickel Catalyst," *ibid.*, 13, 395 (1967).

Jenkins, G. I., and E. K. Rideal, "The Catalytic Hydrogenation of Ethylene at a Nickel Surface," *J. Chem. Soc.*, 3, 2490 (1955).

Kato, K., H. Arai, and U. Ito, "Fluid Flow Model for a Packed-Fluidized Bed," *Chem. React. Eng., Adv. Chem. Ser.*, 271 (1974).

Kato, K., N. Takeuchi, U. Ito, and H. Kubota, "Hydrogenation of Ethylene in a Packed-Fluidized Bed," *J. Chem. Eng. Japan*, 2, 204 (1969).

Koestenblatt, S., "Hydrogenation of Ethylene in a Fluidized Packed Bed," Ph.D. thesis, Polytech. Inst. Brooklyn, New York (1970).
———, and E. N. Ziegler, "Kinetics and Deactivation on Large Catalytic Particles," *AIChE J.*, **17**, 891 (1971).
Koo, L. C. T., "Dispersion in an Interstitially Fluidized-Packed Bed," Ph.D. thesis, Polytech. Inst. Brooklyn, New York (1971).
Pauls, A. C., E. W. Comings, and J. M. Smith, "Kinetics of Hydrogenation of Ethylene on a Nickel Catalyst," *AIChE J.*, **5**, 453 (1959).
Resnick, W., and R. R. White, "Mass Transfer in Systems of Gas and Fluidized Solids," *Chem. Eng. Progr.*, **45**, 377 (1949).
Sane, P. P., R. E. Eckert and J. M. Woods, "On Fitting Combined Integral and Differential Reaction Kinetic Data. Rate Modeling for Catalytic Hydrogenation of Butadiene," *Ind. Eng. Chem. Fundamentals*, **13**, 52 (1974).
Sinfelt, J. H., "A Simple Experimental Method for Catalytic Kinetic Studies," *Chem. Eng. Sci.*, **23**, 1181 (1968).
Van Heerden, C., A. P. P. Nobel, and D. W. Van Krevelen, "Mechanism of Heat Transfer in Fluidized Beds," *Ind. Eng. Chem.*, **45**, 1237 (1953).
Volk, W., C. A. Johnson, and H. H. Stotler, "Effect of Reactor Internals on Quality of Fluidization," *Chem. Eng. Progr.*, **58**, No. 3, 44 (1962).
Wilke, C. R., "Diffusional Properties of Multicomponent Gases," *ibid.*, **46**, No. 2, 95 (1950).
Yoshida, F., D. Ramaswami, and O. A. Hougen, "Temperatures and Partial Pressures at the Surfaces of Catalyst Particles," *AIChE J.*, **8**, 5 (1962).
Ziegler, E. N., "The Interstitial Fluid Bed Reactor," *Chemtech.*, **2**, 690 (1972).
———, and W. T. Brazelton, "Mechanism of Heat Transfer to a Fixed Surface in a Fluidized Bed," *Ind. Eng. Chem. Fundamentals*, **3**, 94 (1964).
Ziegler, E. N., and J. T. Holmes, "Mass Transfer from Fixed Surfaces to Gas Fluidized Beds," *Chem. Eng. Sci.*, **21**, 117 (1966).

Manuscript received April 24, 1978; revision received October 30, and accepted January 22, 1979.

The Simulation of Binary Adsorption in Continuous Countercurrent Operation and a Comparison with Other Operating Modes

A. I. LIAPIS
and
D. W. T. RIPPIN
Eidgenossische Technische Hochschule
Technisch-Chemisches Laboratorium
CH-8092 Zurich (Switzerland)

Simulation studies are presented of three different modes of operating a two-component adsorption system. The efficiency with which an activated carbon adsorbent is utilized is compared for a single fixed bed, a periodic countercurrent system in which the adsorbent is equally distributed over two, four, and six beds and a continuous countercurrent system. The carbon utilization in the single fixed bed was shown to be one third to one half of that in a continuous countercurrent adsorber of the same length, whereas the periodic countercurrent system achieved a utilization of 79 to 98% of that in the continuous system.

The mathematical models used to describe the three different modes of column operation include the effects of axial diffusion in the columns, mass transfer resistance in the boundary layer surrounding each particle, and fluid diffusion within the porous particles.

SCOPE

Although multicomponent adsorption is often encountered in industrial application, most of the studies concerning sorption processes have dealt primarily with systems containing one adsorbable species. Svedberg (1976) reports results on single component adsorption performance from the simulation of fixed bed, periodic, and continuous countercurrent operation with film plus pore diffusion and a linear isotherm.

When more than one component is adsorbed, the shape of the concentration profiles in the adsorber will change radically, giving peaks and plateaus which result from interactions between the adsorbed solutes (Hsieh et al., 1977; Klaus et al., 1977; Liapis and Rippin, 1978) and cannot be modeled by the assumption of linear isotherms. Klaus et al. (1977) report simulated results for two-component adsorption in periodic countercurrent operation for a two-bed system with film mass transfer resistance but in which diffusional effects are neglected. Their results show that with periodic countercurrent operation, carbon utilization is much higher than with a fixed-bed arrangement.

The purpose of the work described here was to simulate multicomponent adsorption on activated carbon in fixed bed periodic and continuous countercurrent operation in order to compare carbon utilization under the three different contacting modes. The models used include film mass transfer and diffusional resistances. The continuous countercurrent operation is theoretically the most efficient procedure but is difficult to realize in practice (Hiester et al., 1954; Westermark, 1975). It was therefore of interest to determine how closely the performance of the periodic countercurrent adsorber would approach that of the continuous system.

A. I. Liapis is at Texas A & M University, College Station, Texas 77843.